

Variational analysis of mass spectra and decay constants for ground state pseudoscalar and vector mesons in the light-front quark model

Ho-Meoyng Choi,¹ Chueng-Ryong Ji,² Ziyue Li,² and Hui-Young Ryu¹

¹*Department of Physics, Teachers College, Kyungpook National University, Daegu, Korea 702-701*

²*Department of Physics, North Carolina State University, Raleigh, North Carolina 27695-8202, USA*

(Received 15 September 2015; published 13 November 2015)

Using the variational principle, we compute mass spectra and decay constants of ground state pseudoscalar and vector mesons in the light-front quark model (LFQM) with the QCD-motivated effective Hamiltonian including the hyperfine interaction. By smearing out the Dirac δ function in the hyperfine interaction, we avoid the issue of negative infinity in applying the variational principle to the computation of meson mass spectra and provide analytic expressions for the meson mass spectra. Our analysis with the smeared hyperfine interaction indicates that the interaction for the heavy meson sector including the bottom and charm quarks gets more point-like. We also consider the flavor mixing effect in our analysis and determine the mixing angles from the mass spectra of (ω, ϕ) and (η, η') . Our variational analysis with the trial wave function including the two lowest order harmonic oscillator basis functions appears to improve the agreement with the data of meson decay constants and the heavy meson mass spectra over the previous computation handling the hyperfine interaction as perturbation.

DOI: [10.1103/PhysRevC.92.055203](https://doi.org/10.1103/PhysRevC.92.055203)

PACS number(s): 12.39.Ki, 12.38.Lg, 13.25.-k, 14.40.-n

I. INTRODUCTION

Effective degrees of freedom to describe a strongly interacting system of hadrons have been one of the key issues in understanding the nonperturbative nature of QCD in the low energy regime. Within an impressive array of effective theories available nowadays, the constituent quark model has been quite useful in providing a good physical picture of hadrons just like the atomic model for the system of atoms. Absorbing the complicated effect of quark, antiquark, and gluon interactions into the effective constituent degrees of freedom, one may make the problem more tractable yet still keep some key features of the underlying QCD to provide useful predictions [1]. The effective potentials used in constituent quark models are typically described by the flux tube configurations generated by the gluon fields as well as the effective “one-gluon-exchange” calculation in QCD [2,3]. In the QCD-motivated effective Hamiltonian, a proper way of dealing with the relativistic effects in the hadron system is quite essential due to the nature of strong interactions. In particular, proper care and handling of relativistic effects has been emphasized in describing the hadrons made of u , d , and s quarks and antiquarks.

As a proper way of handling relativistic effects, the light-front quark model (LFQM) [4–8] appears to be one of the most efficient and effective tools in hadron physics as it takes advantage of the distinguished features of the light-front dynamics (LFD) [9,10]. In particular, the LFD carries the maximum number (seven) of the kinetic (or interaction independent) generators and thus the less effort in dynamics is necessary in order to get the QCD solutions that reflect the full Poincaré symmetries. Moreover, the rational energy-momentum dispersion relation of LFD, namely $p^- = (\mathbf{p}_\perp^2 + m^2)/p^+$, yields the sign correlation between the light-front (LF) energy $p^- (= p^0 - p^3)$ and the LF longitudinal momentum $p^+ (= p^0 + p^3)$ and leads to the suppression of quantum fluctuations of the vacuum, sweeping the complicated

vacuum fluctuations into the zero modes in the limit of $p^+ \rightarrow 0$ [11–13]. This simplification is a remarkable advantage in LFD and facilitates the partonic interpretation of the amplitudes. Based on the advantages of the LFD, the LFQM has been developed [14] and subsequently applied for various meson phenomenologies such as the mass spectra of both heavy and light mesons [15], the decay constants, distribution amplitudes, form factors, and generalized parton distributions [10,14–23].

Despite these successes in reproducing the general features of the data, however, it has proved very difficult to obtain direct connection between the LFQM and QCD. Typically, rigorous derivations of the connection between the effective constituent degrees of freedom and the fundamental QCD quark, antiquark, and gluon degrees of freedom have been explored by solving momentum-dependent mass gap equations as discussed in many-body Hamiltonian approach [24], Dyson-Schwinger approach [25], etc. Although one has not yet explored solving the momentum-dependent mass gap equation in LFD, there has been some attempt to derive an effective LF Hamiltonian starting from QCD using the discrete light-cone quantization (DLCQ) and solve the corresponding equation of motion approximately for the quark and antiquark bound states to provide semianalytical expressions for the masses of pseudoscalar and vector mesons [26]. The attempt to link between QCD and LFQM is also supported by our recent analyses of quark-antiquark distribution amplitudes for pseudoscalar and vector mesons in LFQM [27], where we presented a self-consistent covariant description of twist 2 and twist 3 quark-antiquark distribution amplitudes for pseudoscalar and vector mesons in LFQM to discuss the link between the chiral symmetry of QCD and the LFQM. Our results for the pseudoscalar and vector mesons [27] effectively indicated that the constituent quark and antiquark in the LFQM could be considered as the dressed constituents including the zero-mode quantum fluctuations from the QCD vacuum. Moreover, the light-front holography based on the five-dimensional anti-de Sitter (AdS) space-time and the

conformal symmetry has given insight into the nature of the effective confinement potential and the resulting light front wave functions for both light and heavy mesons [28]. As we have shown in Ref. [29], our LFQM analysis of the pion form factor provided compatible results both in spacelike and timelike regions with the holographic approach to LF QCD [30]. These developments motivate our present work for the more-in-depth analysis of the mass spectra and decay constants for the ground state pseudoscalar and vector mesons in LFQM.

In LFQM, the LF wave function is independent of all reference frames related by the front-form boosts because the longitudinal boost operator as well as the LF transverse boost operators are all kinematical. This is clearly an advantageous feature unique to LFQM, which makes the calculation of observables, such as mass spectra, decay constants, form factors, etc., much more effective. Computing the meson mass spectra, however, we have previously [14,15] treated the hyperfine interaction as a perturbation rather than including it in the variation procedure to avoid the negative infinity from the Dirac δ function contained in the hyperfine interaction. In the present work, we smear out the Dirac δ function by a Gaussian distribution and resolve the infinity problem when variational principle is applied to the hyperfine interaction. We obtain optimal model parameters in our variational analysis including the hyperfine interaction and examine if it improves phenomenologically our numerical results compared to the ones obtained by the perturbative treatment of the hyperfine interaction. For our trial wave function, we also take a larger harmonic oscillator (HO) basis to see if it provides any phenomenological improvement in our predictions of mass spectra and decay constants for ground state pseudoscalar and vector mesons.

The paper is organized as follows. In Sec. II, we describe our QCD-motivated effective Hamiltonian with the smeared-out hyperfine interaction. Using the mixture of the two lowest order HO states as our trial wave function of the variational principle, we find the analytic formula of the mass eigenvalues for the ground state pseudoscalar and vector mesons. The optimum values of model parameters are also presented in this section. In Sec. III, we present our numerical results of the mass spectra obtained by taking a larger HO basis in the trial wave function and compare them with the experimental data as well as our previous calculations [14,15]. To test our trial wave function with the parameters obtained from the variational principle, we also calculate the meson decay constants and compare them with the experimental data as well as other available theoretical predictions. Summary and conclusion follow in Sec. IV. The detailed procedure of fixing our parameters through variational principle is presented in the Appendix.

II. MODEL DESCRIPTION

As mentioned in the Introduction, there has been an attempt to derive an effective LF Hamiltonian starting from QCD using DLCQ [26]. Transforming the LFD variables to the ordinary variables in the instant form dynamics (IFD), one may see the equivalence between the resulting effective LF Hamiltonian for the quark and antiquark bound states and the usual relativistic

constituent quark model Hamiltonian for mesons typically given in the rest frame of the meson, i.e., the center of mass (c.m.) frame for the constituent quark and antiquark system. It may be more intuitive to express the effective LF Hamiltonian describing the relativistic constituent quark model system for mesons in terms of the ordinary IFD variables. Effectively, the meson system at rest is then described as an interacting bound system of effectively dressed valence quark and antiquark typically given by the following QCD-motivated effective Hamiltonian in the quark and antiquark c.m. frame [14,15]:

$$H_{\text{c.m.}} = \sqrt{m_q^2 + \vec{k}^2} + \sqrt{m_{\bar{q}}^2 + \vec{k}^2} + V, \quad (1)$$

where $\vec{k} = (\mathbf{k}_\perp, k_z)$ is the relativistic three-momentum of the constituent quarks and V is the effective potential between quark and antiquark in the rest frame of the meson. The effective potential V is typically given by the linear confining potential V_{conf} plus the effective one-gluon-exchange potential V_{oge} . For S -wave pseudoscalar and vector mesons, the effective one-gluon-exchange potential reduces to the Coulomb potential V_{Coul} plus the hyperfine interaction V_{hyp} . Thus, one may summarize V as

$$V = V_{\text{conf}} + V_{\text{oge}} = a + b r - \frac{4\alpha_s}{3r} + \frac{2 \mathbf{S}_q \cdot \mathbf{S}_{\bar{q}}}{3 m_q m_{\bar{q}}} \nabla^2 V_{\text{Coul}}, \quad (2)$$

where α_s is the strong interaction coupling constant,¹ $\langle \mathbf{S}_q \cdot \mathbf{S}_{\bar{q}} \rangle = 1/4$ ($-3/4$) for the vector (pseudoscalar) meson, and $\nabla^2 V_{\text{Coul}} = (16\pi\alpha_s/3)\delta^3(\mathbf{r})$. Reduction of the LF Hamiltonian in QCD to a similar form of the effective Hamiltonian in the c.m. frame of the quark and antiquark system given by Eqs. (1) and (2) was discussed in Ref. [26]. For the hyperfine interaction V_{hyp} , one may consider the relativization such as $V_{\text{hyp}} \rightarrow \sqrt{m_q m_{\bar{q}}/E_q E_{\bar{q}}} V_{\text{hyp}} \sqrt{m_q m_{\bar{q}}/E_q E_{\bar{q}}}$ [31,32]. Such relativization may be important for the $\delta^3(\mathbf{r})$ -type potential without any smearing in computing particularly the light meson sector. Since we apply the variational principle even for the hyperfine interaction in this work smearing out the Dirac δ function to resolve the infinity problem, we naturally introduce a smearing parameter which may effectively compensate the factor due to the relativization. With this treatment, we are able to provide explicit analytic expressions for the meson mass spectra [see Eq. (9)].

While the effective bound-state mass square $M_{q\bar{q}}^2$ is given by $M_{q\bar{q}}^2 = (P_{\text{c.m.}}^0)^2$ in the c.m. frame of the constituent quark and antiquark system, the energy-momentum dispersion relation in LFD is given by $M_{q\bar{q}}^2 = P^+ P^- - \mathbf{P}_\perp^2$, where the four-momentum of the bound system is denoted by $P^\mu = (P^+, P^-, \mathbf{P}_\perp) = (P^0 + P^3, P^0 - P^3, \mathbf{P}_\perp)$. From this, one may consider the LFQM mass square operator $\hat{P}^+ \hat{P}^- - \hat{\mathbf{P}}_\perp^2$ (that provides the eigenvalues $P^+ P^- - \mathbf{P}_\perp^2$) as the square of the

¹Although one may consider a running coupling constant, we take α_s as one of the variation parameters in this work.

effective Hamiltonian given by Eq. (1), i.e., $H_{\text{c.m.}}^2$. Since the eigenvalues and the expectation values are same for the eigenstates, we compute the expectation value $\langle H_{\text{c.m.}} \rangle$ using the variation principle. Alternatively, one may consider computing the expectation value $\langle H_{\text{c.m.}}^2 \rangle$ in view of the LFQM mass square operator $\hat{P}^+ \hat{P}^- - \hat{\mathbf{P}}_{\perp}^2$ being $\langle H_{\text{c.m.}}^2 \rangle$. Although $\langle (\Delta H_{\text{c.m.}})^2 \rangle = 0$ in principle for the eigenstates, it may be interesting to examine numerically how small the corresponding deviation $\langle (\Delta H_{\text{c.m.}})^2 \rangle = \langle H_{\text{c.m.}}^2 \rangle - \langle H_{\text{c.m.}} \rangle^2$ is. More future works complementary to our present computation of $\langle H_{\text{c.m.}} \rangle$ can be suggested in variational analysis. In this work, we examine the χ^2 values of our computational results in comparison with experimental data to get optimal parameter values in the $\langle H_{\text{c.m.}} \rangle$ computation. This will provide useful ground information for any alternative and/or further works beyond the present analysis.

As discussed earlier, the longitudinal boost operator as well as the LF transverse boost operators are all kinematical and thus the LF wave function does not depend on the external momentum, i.e., P^+ and \mathbf{P}_{\perp} . In effect, the determination of the LF wave function in the meson rest frame such as $P^+ = M_{q\bar{q}}$ and $\mathbf{P}_{\perp} = 0$ will not hinder its use for any other values of P^+ and \mathbf{P}_{\perp} . This provides the applicability of LFQM for the computation of observables beyond the meson mass spectra.

The wave function is thus represented by the Lorentz invariant internal variables $x_i = p_i^+ / P^+$, $\mathbf{k}_{\perp i} = \mathbf{p}_{\perp i} - x_i \mathbf{P}_{\perp}$, and helicity λ_i , where p_i^{μ} is the momenta of constituent quarks. Explicitly, the LF wave function of the ground state mesons is given by

$$\Psi_{100}^{JJ_z}(x_i, \mathbf{k}_{\perp i}, \lambda_i) = \mathcal{R}_{\lambda_q \lambda_{\bar{q}}}^{JJ_z}(x_i, \mathbf{k}_{\perp i}) \Phi(x_i, \mathbf{k}_{\perp i}), \quad (3)$$

where Φ is the radial wave function and $\mathcal{R}_{\lambda_q \lambda_{\bar{q}}}^{JJ_z}$ is the interaction-independent spin-orbit wave function. The spin-orbit wave functions for pseudoscalar and vector mesons are given by [14,33]

$$\begin{aligned} \mathcal{R}_{\lambda_q \lambda_{\bar{q}}}^{00} &= \frac{-\bar{u}_{\lambda_q}(p_q) \gamma_5 v_{\lambda_{\bar{q}}}(p_{\bar{q}})}{\sqrt{2} \sqrt{M_0^2 - (m_q - m_{\bar{q}})^2}}, \\ \mathcal{R}_{\lambda_q \lambda_{\bar{q}}}^{1J_z} &= \frac{-\bar{u}_{\lambda_q}(p_q) [\not{\epsilon}(J_z) - \frac{\epsilon \cdot (p_q - p_{\bar{q}})}{M_0 + m_q + m_{\bar{q}}}] v_{\lambda_{\bar{q}}}(p_{\bar{q}})}{\sqrt{2} \sqrt{M_0^2 - (m_q - m_{\bar{q}})^2}}, \end{aligned} \quad (4)$$

where $\epsilon^{\mu}(J_z)$ is the polarization vector of the vector meson and the boost invariant meson mass squared M_0^2 obtained from the free energies of the constituents is given by

$$M_0^2 = \frac{\mathbf{k}_{\perp}^2 + m_q^2}{x} + \frac{\mathbf{k}_{\perp}^2 + m_{\bar{q}}^2}{1-x}. \quad (5)$$

The spin-orbit wave functions satisfy the relation $\sum_{\lambda_q \lambda_{\bar{q}}} \mathcal{R}_{\lambda_q \lambda_{\bar{q}}}^{JJ_z \dagger} \mathcal{R}_{\lambda_q \lambda_{\bar{q}}}^{JJ_z} = 1$ for both pseudoscalar and vector mesons.

To use a variational principle, we take our trial wave function as an expansion of the true wave function in the HO basis. We use the same trial wave function expanded with the two lowest order HO wave functions $\Phi = \sum_{n=1}^2 c_n \phi_{nS}$ for

both pseudoscalar and vector mesons, where

$$\phi_{1S}(x_i, \mathbf{k}_{\perp i}) = \frac{4\pi^{3/4}}{\beta^{3/2}} \sqrt{\frac{\partial k_z}{\partial x}} e^{-\frac{\vec{k}^2}{2\beta^2}}, \quad (6)$$

$$\phi_{2S}(x_i, \mathbf{k}_{\perp i}) = \frac{4\pi^{3/4}}{\sqrt{6}\beta^{7/2}} (2\vec{k}^2 - 3\beta^2) \sqrt{\frac{\partial k_z}{\partial x}} e^{-\frac{\vec{k}^2}{2\beta^2}}, \quad (7)$$

and β is the variational parameter. We should note here that our LF wave functions ϕ_{nS} are dependent on M_0^2 and thus cannot be factorized into a function of $\mathbf{k}_{\perp i}$ multiplied by another function of x_i . In particular, \vec{k}^2 in Eqs. (6) and (7) is given by $\vec{k}^2 = \mathbf{k}_{\perp}^2 + k_z^2$, where $k_z = (x - 1/2)M_0 + (m_q^2 - m_{\bar{q}}^2)/2M_0$. For instance, $e^{-\vec{k}^2/2\beta^2} = e^{m^2/2\beta^2} e^{-M_0^2/8\beta^2}$ in the case of equal quark and antiquark mass $m_q = m_{\bar{q}} = m$. The variable transformation $(x, \mathbf{k}_{\perp}) \rightarrow \vec{k} = (\mathbf{k}_{\perp}, k_z)$ requires the Jacobian factor given by $\partial k_z / \partial x = M_0 [1 - (m_q^2 - m_{\bar{q}}^2)/M_0^2] / 4x(1-x)$ as one can see from Eqs. (6) and (7). The normalization of the wave function ϕ_{nS} is thus given by

$$\int_0^1 dx \int \frac{d^2 \mathbf{k}_{\perp}}{16\pi^3} |\phi_{nS}(x_i, \mathbf{k}_{\perp i})|^2 = 1. \quad (8)$$

With $\Phi = \sum_{n=1}^2 c_n \phi_{nS}$, we evaluate the expectation value of the Hamiltonian in Eq. (1), i.e., $\langle \Phi | H_{\text{c.m.}} | \Phi \rangle$ which depends on the variational parameter β . According to the variational principle, we can set the upper limit of the ground state's energy by calculating the expectation value of the system's Hamiltonian with a trial wave function. In our previous calculations [14,15], which we call "CJ model", we first evaluate the expectation value of the central Hamiltonian $T + V_{\text{conf}} + V_{\text{coul}}$ with the trial function ϕ_{1S} , where T is the kinetic energy part of the Hamiltonian. Once the model parameters are fixed by minimizing the expectation value $\langle \phi_{1S} | (T + V_{\text{conf}} + V_{\text{Coul}}) | \phi_{1S} \rangle$, then the mass eigenvalue of each meson is obtained as $M_{q\bar{q}} = \langle \phi_{1S} | H_{\text{c.m.}} | \phi_{1S} \rangle$. The hyperfine interaction V_{hyp} in CJ model, which contains a Dirac δ function, was treated as perturbation to the Hamiltonian and was left out in the variational process that optimizes the model parameters. The main reason for doing this was to avoid the negative infinity generated by the δ function as was pointed out in [31]. Specifically, $\langle \phi_{1S} | V_{\text{hyp}} | \phi_{1S} \rangle$ for pseudoscalar mesons decreases faster than other terms that increase as β increases and the expectation value of the Hamiltonian is unbounded from below.

The singular nature of the hyperfine interaction and its regularization is a standard topic in atomic physics and the atomic analysis has been carried out to extraordinary precision [34]. In particular, a Bethe-Salpeter based bound-state formalism was applied to the calculation of recoil contributions of order $m\alpha^6$ to hyperfine splitting in ground-state positronium [35]. Instead of dropping the relative energy dependence in favor of equations with a simpler kinematical structure but a more complicated effective kernel, the Barbieri-Remiddi formalism [36] was discussed as an effective way to handle significant complications concerning the Bethe logarithm [37]. As discussed in Ref. [35], the δ function of the relative energy p_0 is replaced by a smearing function of p_0 in the Barbieri-Remiddi formalism [36]. In LFD, the equal LF time x^+ ($= x^0 + x^3$) correlates the ordinary time x^0 and space x^3 so

that the idea of smearing p^0 in the Barbieri-Remiddi formalism may be extended to smear the $\delta^3(\mathbf{r})$ function in hyperfine interaction discussed in the present work. In this respect, our regularization procedure discussed below would also be valid and is compatible for the hyperfine splitting in atoms. Analytic treatment of positronium spin splittings was presented in LF QED [38] and more recent DLCQ application to the analysis of $\mu^+\mu^-$ bound state spectrum can be found in Ref. [39].

To avoid the negative infinity, we thus use a Gaussian smearing function to weaken the singularity of $\delta^3(\mathbf{r})$ in hyperfine interaction, viz. [31,32], $\delta^3(\mathbf{r}) \rightarrow (\sigma^3/\pi^{3/2})e^{-\sigma^2\mathbf{r}^2}$.

Once the δ function is smeared out like this, a true minimum for the mass occurs at a certain value of β . The analytic formulas of mass eigenvalues for our modified Hamiltonian with the smeared-out hyperfine interaction, i.e., $M_{q\bar{q}} = \langle \Phi | H_{c.m.} | \Phi \rangle$, are found as follows²:

$$\begin{aligned}
M_{q\bar{q}} = & a + \frac{b}{\beta\sqrt{\pi}} \left(3 - c_1^2 - 2\sqrt{\frac{2}{3}}c_1c_2 \right) \\
& + \frac{\beta}{\sqrt{\pi}} \sum_{i=q,\bar{q}} \left\{ \sqrt{\pi}(\sqrt{6}c_1c_2 - 3c_2^2)U\left(-\frac{1}{2}, -2, z_i\right) \right. \\
& + \frac{1}{3}c_2^2z_i^2e^{\frac{z_i}{2}}(3 - z_i)K_2\left(\frac{z_i}{2}\right) \\
& + \left. \frac{1}{6}z_ie^{\frac{z_i}{2}}(2c_2^2z_i^2 - 3c_1^2 - 6\sqrt{6}c_1c_2 + 9)K_1\left(\frac{z_i}{2}\right) \right\} \\
& - \frac{4\alpha_s\beta}{9\sqrt{\pi}} \left\{ 5 + c_1^2 + 6\sqrt{2/3}c_1c_2 \right. \\
& - \frac{4\beta^2\sigma^3\langle \mathbf{S}_q \cdot \mathbf{S}_{\bar{q}} \rangle}{(\beta^2 + \sigma^2)^{7/2}m_qm_{\bar{q}}} \left[(2\sqrt{6}c_1c_2 + 3 - c_1^2)\sigma^4 \right. \\
& \left. \left. + 2\beta^2(2c_1^2 + \sqrt{6}c_1c_2)\sigma^2 + 2\beta^4 \right] \right\}, \quad (9)
\end{aligned}$$

where $z_i = m_i^2/\beta^2$ and K_1 is the modified Bessel function of the second kind and $U(a,b,z)$ is Tricomi's (confluent hypergeometric) function. We should note that the mass formula for the δ -function hyperfine interaction corresponds to Eq. (9) in the limit of $\sigma \rightarrow \infty$. We then apply the variational principle, i.e., $\partial M_{q\bar{q}}/\partial\beta = 0$, to find the optimal model parameters in order to get a best fit for the mass spectra of ground state pseudoscalar and vector mesons (a more detailed description of this procedure can be found in the Appendix).

Our optimized potential parameters are obtained as $\{a = -0.6699 \text{ GeV}, b = 0.18 \text{ GeV}^2, \alpha_s = 0.4829\}$. For the best fit of the ground state mass spectra, we obtain $c_1 = +\sqrt{0.7}$ and $c_2 = +\sqrt{0.3}$. We should note that our potential parameters are quite comparable with the ones suggested by Scora and Isgur [40], where they obtained $a = -0.81 \text{ GeV}, b = 0.18 \text{ GeV}^2$,

TABLE I. Constituent quark masses [GeV] and the smearing parameter σ [GeV] obtained by the variational principle for the Hamiltonian with a smeared-out hyperfine interaction. Here $q = u$ and d .

m_q	m_s	m_c	m_b	σ
0.205	0.380	1.75	5.15	0.423

and $\alpha_s = 0.3 \sim 0.6$. For a comparison, the coupling constant we found in our previous CJ model [14,15] was $\alpha_s = 0.31$.

While we use the common potential parameters (a,b,α_s) for all the mesons, it was shown in [32,41] that if a smearing procedure for the $\delta^3(\mathbf{r})$ function is used, then a large Gaussian parameter σ is obtained for the heavy quark sector. In our updated potential model using the smeared hyperfine interaction $(\sigma^3/\pi^{3/2})e^{-\sigma^2\mathbf{r}^2}$, we also confirm the same observation as in [32] for the heavy meson sector including (b,c) quarks. Thus, we differentiate the smearing parameter σ for the heavy (b,c) sectors such as $(c\bar{c}, b\bar{c}, b\bar{b})$ from the other $(q\bar{q})$ sectors by introducing multiplicative factor in front of σ , i.e., $\sigma \rightarrow \lambda\sigma$ with $\lambda > 1$, while other potential parameters (a,b,α_s) remain the same for all $(q\bar{q})$ sectors. This differentiation is to accommodate the hyperfine splittings for the heavy (b,c) quark sectors as we will show in the next section. Our new updated results with λ differentiation using the common potential parameters (a,b,α_s,σ) for all meson sectors show definite improvement in the χ^2 fit of the experimental data for meson masses.

Our optimal constituent quark masses and the smearing parameters σ are listed in Table I. Since we included the hyperfine interaction with smearing function entirely in our variational process, we now obtain the two different sets of β values, one for pseudoscalar and the other for vector mesons, respectively. The optimal Gaussian parameters $\beta_{q\bar{q}}$ for pseudoscalar and vector mesons are also listed in Table II. We should note that the values of the multiplicative factor λ to get the best fits for the mass eigenvalues are obtained as $\lambda = (2, 2.3, 3)$ for $(c\bar{c}, b\bar{c}, b\bar{b})$ sectors. As a sensitivity check, however, we present the numerical results with the following theoretical error bars $\lambda = (2_{-1}^{+1}, 2.3_{-1}^{+1}, 3_{-2}^{+2})$ for $(c\bar{c}, b\bar{c}, b\bar{b})$ sectors, respectively. Although one may fine-tune more to improve the hyperfine splittings for the heavy-light sectors by using different set of λ parameters, we set $\lambda = 1$ for any other $q\bar{q}$ sectors except $(c\bar{c}, b\bar{c}, b\bar{b})$ sectors in this work for simplicity.

We also determine the mixing angles from the mass spectra of (ω, ϕ) and (η, η') . Identifying $(\mathcal{F}, \mathcal{F}') = (\phi, \omega)$ and (η, η') for vector and pseudoscalar nonets, the flavor assignment of \mathcal{F} and \mathcal{F}' mesons in the quark-flavor basis $n\bar{n} = (u\bar{u} + d\bar{d})/\sqrt{2}$ and $s\bar{s}$ is given by [42–44]

$$\begin{pmatrix} \mathcal{F} \\ \mathcal{F}' \end{pmatrix} = \begin{pmatrix} \cos \alpha & -\sin \alpha \\ \sin \alpha & \cos \alpha \end{pmatrix} \begin{pmatrix} n\bar{n} \\ s\bar{s} \end{pmatrix} = U(\alpha) \begin{pmatrix} n\bar{n} \\ s\bar{s} \end{pmatrix}, \quad (10)$$

where α is the mixing angle in the quark-flavor basis. For the $\eta - \eta'$ mixing, the SU(3) mixing angle θ in the flavor SU(3) octet-singlet basis (η_8, η_1) can also be used and the relation between the mixing angles is given by $\theta = \alpha - \arctan\sqrt{2} \simeq$

²Although the true minimum occurs with the smeared-out hyperfine interaction even for ϕ_{1S} case, we found that the phenomenological results do not show any significant improvement compared to CJ model.

TABLE II. The Gaussian parameter β [GeV] for ground state pseudoscalar ($J^{PC} = 0^{-+}$) and vector (1^{--}) mesons obtained by the variational principle. $q = u$ and d . We should note that $\lambda = (2_{-1}^{+1}, 2.3_{-1}^{+1}, 3_{-2}^{+2})$ are used to get $(\beta_{cc}, \beta_{bc}, \beta_{bb})$ values and $\lambda = 1$ is used to get the rest of β_{qq} values.

J^{PC}	β_{qq}	β_{qs}	β_{ss}	β_{qc}	β_{cs}	β_{cc}	β_{qb}	β_{bs}	β_{bc}	β_{bb}
0^{-+}	0.4465	0.3759	0.3445	0.3801	0.3859	$0.5270_{-0.0235}^{+0.0291}$	0.4226	0.4412	$0.6646_{-0.0174}^{+0.0219}$	$0.9906_{-0.0223}^{+0.0420}$
1^{--}	0.2346	0.2598	0.2820	0.3445	0.3667	$0.4914_{+0.0072}^{-0.0062}$	0.4057	0.4321	$0.6365_{+0.0056}^{-0.0058}$	$0.9603_{+0.0075}^{-0.0122}$

$\alpha = 54.7^\circ$ [45]. Taking into account SU(3) symmetry breaking and using the parametrization for the (mass)² matrix suggested by Scadron [46], we obtain [14]

$$\tan^2 \alpha = \frac{(M_{\mathcal{F}'}^2 - M_{s\bar{s}}^2)(M_{\mathcal{F}}^2 - M_{n\bar{n}}^2)}{(M_{\mathcal{F}}^2 - M_{n\bar{n}}^2)(M_{s\bar{s}}^2 - M_{\mathcal{F}}^2)}, \quad (11)$$

which is the model-independent equation for any $q\bar{q}$ meson nonets. The details of obtaining meson mixing angles using quark-annihilation diagrams are summarized in [14], where the mixing angle $\delta = \alpha - 90^\circ$ is used in the quark-flavor basis. In order to predict the $\omega - \phi$ and $\eta - \eta'$ mixing angles, we use the experimental values of $M_{\mathcal{F}} = (M_\phi, M_\eta)$ and $M_{\mathcal{F}'} = (M_\omega, M_{\eta'})$ as well as the masses of $M_{n\bar{n}}^V [M_{s\bar{s}}^V] = 780$ (901) MeV and $M_{n\bar{n}}^P [M_{s\bar{s}}^P] = 140$ (726) MeV obtained from $\langle \Phi | H_{s\bar{s}} | \Phi \rangle$ for both vector (V) and pseudoscalar (P) mesons, respectively. Our prediction for the $\omega - \phi$ mixing angle is $\alpha_{\omega-\phi} = 84.8^\circ$, which is about 5.2° deviated from the ideal mixing $\alpha_{\text{ideal}}^{\omega-\phi} = 90^\circ$. Our prediction for $\eta - \eta'$ mixing angle is $\alpha_{\eta-\eta'} = 36.3^\circ$, which is in agreement with the range 34.7° to 44.7° of phenomenological values [42,45].

Our updated model with the smeared hyperfine interaction appears to improve the result of the mass spectrum, which is presented in the next section. This may suggest that when using constituent quark models, the contact interactions has to be smeared out in general. In fact, we think this smeared interaction is more consistent with the physical picture for a system of the effective constituent quarks which are not point-like.

For practical application of our model, we also compute the decay constants for the ground state pseudoscalar and vector mesons. The decay constants are typically defined by

$$\begin{aligned} \langle 0 | \bar{q} \gamma^\mu \gamma_5 q | P \rangle &= i f_P P^\mu, \\ \langle 0 | \bar{q} \gamma^\mu q | V(P, h) \rangle &= f_V M_V \epsilon^\mu(h), \end{aligned} \quad (12)$$

for pseudoscalar and vector mesons, respectively. For the η and η' case, one may also define decay constants through matrix elements of octet and singlet axial-vector currents. However, as discussed in [42,43], they cannot be expressed as $U(\theta)\text{diag}[f_8, f_1]$ due to the $U(1)_A$ anomaly. Thus, the following two mixing angle parametrization is adopted [42,43]:

$$\begin{aligned} f_\eta^8 &= f_8 \cos \theta_8, \quad f_\eta^1 = -f_1 \sin \theta_1, \\ f_{\eta'}^8 &= f_8 \sin \theta_8, \quad f_{\eta'}^1 = f_1 \cos \theta_1. \end{aligned} \quad (13)$$

The parameters appearing in Eq. (13) are related to the basis parameters $\alpha, f_q \equiv f_{n\bar{n}}$, and $f_s \equiv f_{s\bar{s}}$, characterizing the

quark-flavor mixing scheme as follows [42]:

$$\begin{aligned} f_8^2 &= \frac{f_q^2 + 2f_s^2}{3}, \quad \theta_8 = \alpha - \arctan\left(\frac{\sqrt{2}f_s}{f_q}\right), \\ f_1^2 &= \frac{2f_q^2 + f_s^2}{3}, \quad \theta_1 = \alpha - \arctan\left(\frac{\sqrt{2}f_q}{f_s}\right). \end{aligned} \quad (14)$$

Using the plus component ($\mu = +$) of the currents, one can calculate the decay constants. The explicit formulas of pseudoscalar and vector meson decay constants in quark-flavor basis are given by [14,33]

$$\begin{aligned} f_P &= \sqrt{6} \int_0^1 dx \int \frac{d^2\mathbf{k}_\perp}{8\pi^3} \frac{\Phi(x, \mathbf{k}_\perp)}{\sqrt{\mathcal{A}^2 + \mathbf{k}_\perp^2}} \mathcal{A}, \\ f_V &= \sqrt{6} \int_0^1 dx \int \frac{d^2\mathbf{k}_\perp}{8\pi^3} \frac{\Phi(x, \mathbf{k}_\perp)}{\sqrt{\mathcal{A}^2 + \mathbf{k}_\perp^2}} \left[\mathcal{A} + \frac{2\mathbf{k}_\perp^2}{D_{\text{LF}}} \right], \end{aligned} \quad (15)$$

where $\mathcal{A} = (1-x)m_q + xm_{\bar{q}}$ and $D_{\text{LF}} = M_0 + m_q + m_{\bar{q}}$.

III. RESULTS AND DISCUSSION

In Fig. 1, we show the masses (and hyperfine splittings) and the corresponding decay constants of heavy quarkonia depending on the variation of the multiplicative factor λ . For $(c\bar{c})$ [Fig. 1(a) and 1(b)] and $(b\bar{b})$ [Fig. 1(c) and 1(d)], we plot the curves corresponding three different λ values, i.e., $\lambda\sigma = (1, 2, 3)\sigma$ and $\lambda\sigma = (1, 3, 5)\sigma$, respectively. The results indicate that the interaction between heavier quarks gets more point-like as the larger λ values are favored in comparison with data. In general, as one can see from Fig. 1, the hyperfine splittings for both charmonium [Fig. 1(a)] and bottomonium [Fig. 1(c)] states increases as λ increases while other potential parameters remain the same. On the other hand, the decay constants of vector mesons decrease while the corresponding decay constants of pseudoscalar mesons increase as λ increases [see Fig. 1(b) and 1(d)]. One may increase λ value even further to have better hyperfine splittings compared to the data. However, one may not increase λ value arbitrarily to accommodate the empirical constraint $f_V \geq f_P$. Similarly, we could improve the hyperfine splitting for $(b\bar{c})$ sector by using $\lambda = 2.3$.

We show in Fig. 2 our prediction of the meson mass spectra obtained from the variational principle to the effective Hamiltonian with the smeared-out hyperfine interaction using the trial function $\Phi = \sum_i^2 c_i \phi_{iS}$ and compare them with the experimental data [45] as well as the results obtained from the CJ model with the linear confining potential [14]. We should note that the (π, ρ) masses are used as inputs. The $(\eta, \eta', \omega, \phi)$ masses are also used as inputs to find the

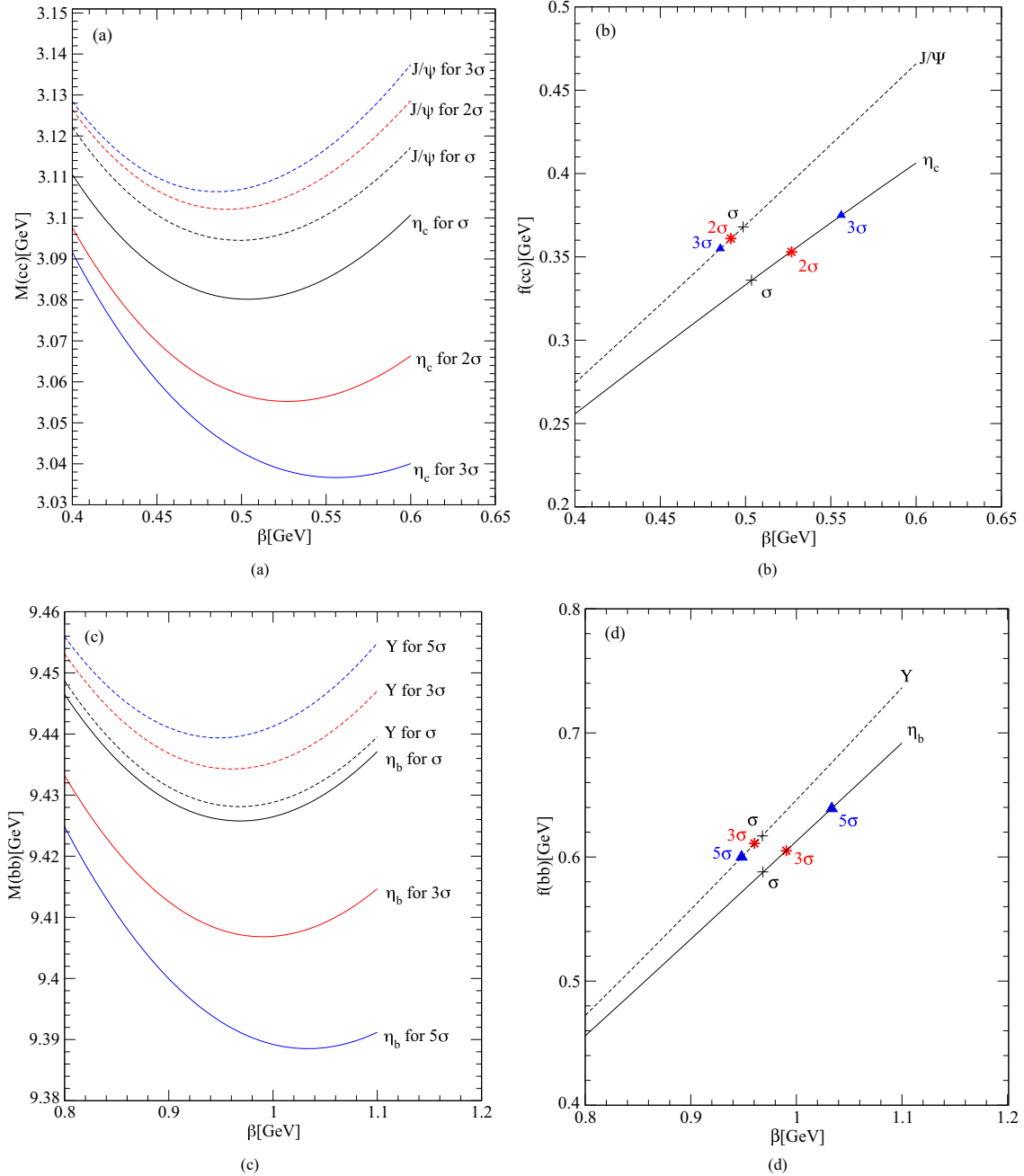


FIG. 1. (Color online) The masses (and hyperfine splittings) and the corresponding decay constants of heavy quarkonia depending on the variation of the multiplicative factor λ , i.e., $(c\bar{c})$ [(a) and (b)] with two different $\lambda\sigma = (1,2)\sigma$ and $(b\bar{b})$ [(c) and (d)] with two different $\lambda\sigma = (1,3)\sigma$ values, respectively.

$(\eta - \eta')$ and $(\omega - \phi)$ mixing angles. The theoretical error bars for $(c\bar{c}, b\bar{c}, b\bar{b})$ sectors are due to the usage of $\lambda = (2_{-1}^{+1}, 2.3_{-1}^{+1}, 3_{-2}^{+2})$ values, respectively. As one can see, our trial wave function Φ including more HO basis generates overall better results than our CJ model. This can be seen from our $\chi^2 = 0.008$ compared to $\chi^2 = 0.012$ obtained from the CJ model [15]. Except the mass of K , our predictions for the masses of $1S$ -state pseudoscalar and vector mesons are within 4% error. Especially, our effective Hamiltonian with the smeared hyperfine interaction using Φ clearly improves the

TABLE III. Decay Constants for light mesons (in unit of MeV) obtained from our updated LFQM.

Model	f_π	f_ρ	f_K	f_{K^*}
This work	130	205	161	224
CJ [16]	130	246	161	256
Exp. [45]	130.4(2)	208 ^a , 216(5) ^b	156.1(8)	217(7)

^aExp. value for $\Gamma(\tau \rightarrow \rho\nu_\tau)$.

^bExp. value for $\rho^0 \rightarrow e^+e^-$.

TABLE IV. Decay constants in the singlet-octet basis and the mixing angle in the quark-flavor basis.

Reference	f_8/f_π	θ_8	f_1/f_π	θ_1	α
This work	1.30	-27.3°	1.16	-8.6°	36.3°
[42]	1.26	-21.2°	1.17	-9.2°	39.3°
[44]	1.28	-20.5°	1.25	-4°	—
[49]	1.51	-23.8°	1.29	-2.4°	40.7°
[50]	1.27	-19.5°	1.17	-5.5°	42.1°

predictions of heavy-light and heavy quarkonia systems such as $(\eta_c, J/\psi, B_c, \eta_b, \Upsilon)$ compared to the CJ model adopting the contact hyperfine interaction. Although the experimental data for B_c^* is not yet available, our predictions of B_c^* , i.e., 6330_{-5}^{+3} MeV, are quite comparable with the lattice prediction $6331(9)$ MeV [47] as well as other quark model predictions such as 6340 MeV [32] and 6345.8 MeV [48].

In Table III, we list our predictions for the decay constants of light mesons (π, K, ρ, K^*) obtained by using the mixed wave function Φ of $1S$ and $2S$ HO states and compare them with the results from the CJ model [16] and the experimental data [45]. As one can see, our updated model calculation including the hyperfine interaction in the variation procedure clearly improves the results over the CJ model.

For the decay constant of the ϕ meson, our prediction for the ideal mixing angle ($\alpha_{\text{ideal}}^{\omega-\phi} = 90^\circ$) is given by $f_\phi = f_{s\bar{s}}^V = 245.1$ MeV. However, we obtain $f_\phi = f_{s\bar{s}}^V = 226$ MeV using our predicted mixing angle $\alpha_{\omega-\phi} = 84.8^\circ$. Comparing to the experimental value $f_\phi^{\text{exp}} = 233$ MeV [45] (extracted from the partial width of $\phi \rightarrow e^+e^-$ decay), our prediction for f_ϕ prefers a rather small $\omega - \phi$ mixing angle such as $\alpha_{\omega-\phi} \simeq 87.5^\circ$ than the ideal mixing.

For the decay constants of η and η' , our predictions of the decay constants f_q and f_s are given by $f_q = 130$ MeV and $f_s = 184.8$ MeV so that $f_q/f_\pi = 1$ and $f_s/f_\pi = 1.42$, where the SU(3) breaking effect is manifest in the ratio $f_q/f_s \neq 1$. Using Eq. (14), we obtain $f_8/f_\pi = 1.30$ and $f_1/f_\pi = 1.16$ with $\theta_8 = -27.3^\circ$ and $\theta_1 = -8.6^\circ$, respectively. In Table IV, we compare our results for the decay constants in the singlet-octet basis and the mixing angle in the quark-flavor basis with other theoretical predictions [42,44,49,50]. As one can see, our results are consistent with other theoretical model results.

 TABLE V. Charmed meson decay constants (in units of MeV) obtained from our updated LFQM. The theoretical error bars for $f_{\eta_c(J/\psi)}$ come from the variation of the smearing parameters σ , i.e., $f_{\eta_c(J/\psi)}(2\sigma_{-\sigma}^{+\sigma})$.

Model	f_D	f_{D^*}	f_{D_s}	$f_{D_s^*}$	f_{η_c}	$f_{J/\psi}$
This work	208	230	231	260	353_{-17}^{+22}	361_{-7}^{+6}
CJ [23]	197	239	232	273	326	360
Lattice [51]	$211 \pm 3 \pm 17$	$245 \pm 20_{-2}^{+3}$	$231 \pm 12_{-1}^{+8}$	$272 \pm 16_{-20}^{+3}$	—	—
QCD [52,53]	208 ± 7 [52]	—	250 ± 7 [52]	—	387 ± 7 [53]	418 ± 9 [53]
Sum rules [55]	201_{-23}^{+12}	242_{-12}^{+20}	238_{-23}^{+13}	293_{-14}^{+19}	—	—
BS [56]	230 ± 25	340 ± 23	248 ± 27	375 ± 24	292 ± 25	459 ± 28
QM [57]	240 ± 20	—	290 ± 20	—	—	—
RQM [58]	234	310	268	315	—	—
Exp	206.7 ± 8.9 [45]	—	257.5 ± 6.1 [45]	—	335 ± 75 [59]	407 ± 5 [45]

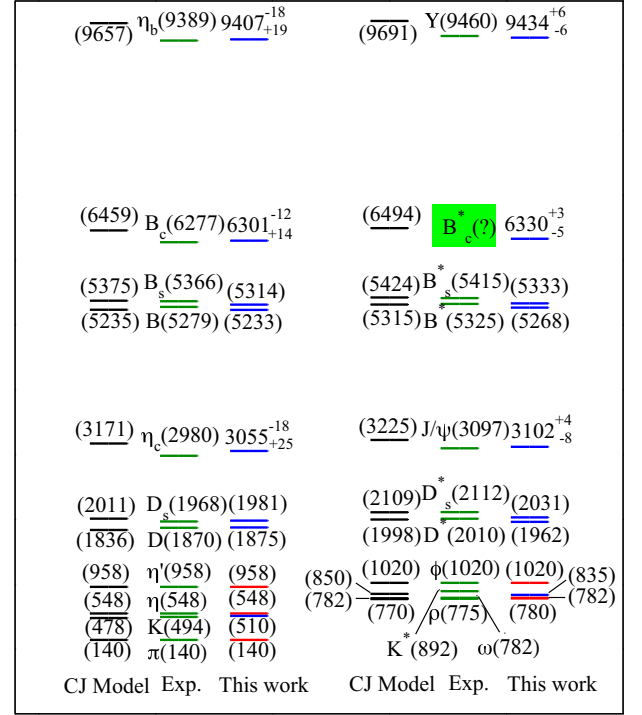


FIG. 2. (Color online) Fit of the ground state meson masses [MeV] with the parameters given in Tables II and I compared with the fit from our previous calculations using the CJ model [15] as well as the experimental values. The (π, ρ) masses are our input data. The $(\eta, \eta', \omega, \phi)$ masses are also used as input to find the $(\eta - \eta')$ and $(\omega - \phi)$ mixing angles. The theoretical error bars for $(c\bar{c}, b\bar{c}, b\bar{b})$ sectors are due to the usage of $\lambda = (2_{-1}^{+1}, 2.3_{-1}^{+1}, 3_{-2}^{+2})$ values, respectively.

Since the experimental values are very well known for light mesons, this improvement is very encouraging.

In Table V, we list our predictions for the charmed meson decay constants $(f_D, f_{D^*}, f_{D_s}, f_{D_s^*}, f_{\eta_c}, f_{J/\psi})$ together with the CJ model [23], lattice QCD [51–54], QCD sum rules [55], relativistic Bethe-Salpeter (BS) model [56], relativized quark model [57], and other relativistic quark model (RQM) [58] predictions as well as the available experimental data [45,59]. We extract the experimental value $(f_{J/\psi})_{\text{exp}} = (407 \pm 5)$ MeV from the data $\Gamma_{\text{exp}}(J/\psi \rightarrow e^+e^-) = (5.55 \pm 0.14)$ keV [45]

TABLE VI. Bottomed meson decay constants (in units of MeV) obtained from our updated LFQM. The theoretical error bars for $f_{\eta_b(\Upsilon)}$ come from the variation of the smearing parameters σ , i.e., $f_{\eta_b(\Upsilon)}(3\sigma_{-2\sigma}^{+2\sigma})$.

Model	f_B	f_{B^*}	f_{B_s}	$f_{B_s^*}$	f_{η_b}	f_Υ
This work	181	188	205	216	605_{-17}^{+32}	611_{+6}^{-11}
CJ [23]	171	185	205	220	507	529
Lattice [51]	$179 \pm 18_{-9}^{+34}$	$196 \pm 24_{-2}^{+39}$	$204 \pm 16_{-0}^{+41}$	$229 \pm 20_{-16}^{+41}$	–	–
QCD [52,60]	189 ± 8 [52]	–	228 ± 8 [52]	–	–	649 ± 31 [60]
Sum rules [55]	207_{-9}^{+17}	210_{-12}^{+10}	242_{-12}^{+17}	251_{-16}^{+14}	–	–
BS [56]	196 ± 29	238 ± 18	216 ± 32	272 ± 20	–	498 ± 20
QM [57]	155 ± 15	–	210 ± 20	–	–	–
RQM [58]	189	219	218	251	–	–
Exp	229_{-31-37}^{+36+34} [61]	–	–	–	–	689 ± 5 [45]

and the formula

$$\Gamma(V \rightarrow e^+e^-) = \frac{4\pi}{3}\alpha_{\text{QED}}^2 e_Q^2 \frac{f_V^2}{M_V}, \quad (16)$$

where e_Q is the electric charge of the heavy quark in units of e ($2/3$ for c and $-1/3$ for b). We should note that our results of the ratios $f_{D_s}/f_D = 1.11$ and $f_{\eta_c}/f_{J/\psi} = 0.98_{-0.07}^{+0.08}$ are quite comparable with the available experimental data, $f_{D_s}/f_D = 1.25 \pm 0.06$ [45] and $f_{\eta_c}/f_{J/\psi} = 0.81 \pm 0.19$ [45,59], respectively. Our result of the ratios $f_{D_s^*}/f_{D^*} = 1.13$ is also in good agreement with other theoretical model calculations such as $1.16 \pm 0.02 \pm 0.06$ from the lattice QCD [54] and 1.10 ± 0.06 from the BS model [56].

We list our results for the bottomed mesons ($f_B, f_{B^*}, f_{B_s}, f_{B_s^*}, f_{\eta_b}, f_\Upsilon$) in Table VI, and compare with the CJ model [23], lattice QCD [51,52,60], QCD sum rules [55], BS model [56], relativized quark model [57], and RQM [58] predictions as well as the available experimental data [45,61]. Note that we extract the experimental value $(f_\Upsilon)_{\text{exp}} = (689 \pm 5)$ MeV from the data $\Gamma_{\text{exp}}(\Upsilon \rightarrow e^+e^-) = 1.340 \pm 0.018$ keV [45] and Eq. (16) with $e_Q^2 = 1/9$ for $V = \Upsilon$. Our results for the ratios $f_{B_s}/f_B = 1.13$ and $f_{B_s^*}/f_{B^*} = 1.15$ are in good agreement with the QCD sum rules [55] predictions: $f_{B_s}/f_B = 1.17_{-0.03}^{+0.04}$ and $f_{B_s^*}/f_{B^*} = 1.20 \pm 0.04$. Ours are also in good agreement with the lattice results, $f_{B_s}/f_B = 1.206(24)$ [52] and $f_{B_s^*}/f_{B^*} = 1.17(4)_{-3}^{+1}$ [51]. Our result for the ratio $f_{\eta_b}/f_\Upsilon = 0.99_{-0.04}^{+0.07}$ is consistent with the heavy quark symmetry $f_{\eta_b}/f_\Upsilon = 1$ [62]. One can also see that for heavy charmed and bottomed mesons, the trial wave function ϕ_B produces better results when compared with the experimental data as well as the lattice results.

In Table VII, we present our model predictions for the decay constants of f_{B_c} and $f_{B_c^*}$, and compare them with other model calculations [15,57,63–67]. Our results are comparable with other model calculations.

TABLE VII. Bottom-charmed meson decay constants (in units of MeV) obtained from our updated LFQM. The theoretical error bars for $f_{B_c(B_c^*)}$ come from the variation of the smearing parameters σ , i.e., $f_{B_c(B_c^*)}(2.3\sigma_{-\sigma}^{+\sigma})$.

Model	This work	CJ [15]	[63]	[64]	[65]	[66]	[67]	[57]
f_{B_c}	389_{-3}^{+16}	349	360	433	500	460 ± 60	517	410 ± 40
$f_{B_c^*}$	391_{+4}^{-5}	369	–	503	500	460 ± 60	517	–

IV. SUMMARY AND CONCLUSION

In this work, we updated our LFQM by smearing out the Dirac δ function in the hyperfine interaction to avoid the issue of negative infinity in applying the variational principle to the computation of meson mass spectra, while our previous model (CJ model) used the perturbation method to handle the δ function in the contact hyperfine interaction. Using the mixed wave function Φ of $1S$ and $2S$ HO states as the trial wave function, we calculated both the mass spectra of the ground state pseudoscalar and vector mesons and the decay constants of the corresponding mesons. The flavor mixing effect has also been implemented for the meson systems of (ω, ϕ) and (η, η') .

The variational analysis with Φ seems to improve the agreement with the data of meson decay constants over the results of the CJ model. It also appears to provide the better agreement with data in the heavy meson mass spectra. Accommodating the empirical constraint $f_V \geq f_P$, we have shown that the mass spectra and the hyperfine splittings for heavy (b, c) quark sector get improved by introducing the multiplicative factor λ in front of the smearing parameter σ , i.e., $\sigma \rightarrow \lambda\sigma$, in the smeared hyperfine interaction $(\sigma^3/\pi^{3/2})e^{-\sigma^2 r^2}$. Our results indicate that the interaction between heavier quarks gets more point-like as the larger λ values are favored in comparison with data. The distinction between the heavy meson sector and the light meson sector is rather natural in our LFQM analyses. To get more definite conclusion in this respect, further analysis of other wave function related observables such as various meson elastic and transition form factors may be useful. It may be also interesting to analyze radially excited meson states using the larger HO basis.

ACKNOWLEDGMENTS

This work is supported by the US Department of Energy (No. DE-FG02-03ER41260). The work of H.-M.C.

was supported in part by the National Research Foundation Grant funded by the Korean Government (NRF-2014R1A1A2057457) and that of Z.L. was supported in part by the JSA/Jefferson Lab fellowship.

APPENDIX: FIXATION OF THE MODEL PARAMETERS USING VARIATIONAL PRINCIPLE

In our model, we assumed SU(2) flavor symmetry and have the following parameters that need to be fixed: constituent quark masses ($m_{u(d)}, m_s, m_c, m_b$), potential parameters (a, b, α_s), gaussian parameter β , and the smearing parameter σ . For our trial wave function $\Phi = \sum_{n=1}^2 c_n \phi_{nS}$, we also have the mixing factor $c_n (n = 1, 2)$ that we have to adjust. Notice that the β values here are not only different for different quark combinations, but also different for pseudoscalar and vector mesons of the same quark combination. The reason for this is that the hyperfine interaction we included in our parametrization process gives different contributions to the masses of pseudoscalar and vector mesons and thus induces different parametrizations under variational principle.

We now illustrate our procedure for fixing these parameters. The variational principle gives us one constraint

$$\frac{\partial \langle \Phi | H | \Phi \rangle}{\partial \beta} = \frac{\partial M_{q\bar{q}}}{\partial \beta} = 0. \quad (\text{A1})$$

We can use this equation to rewrite the coupling constant α_s in terms of other parameters and plug it back into Eq. (9) and thus eliminate α_s . The string tension b is fixed to be 0.18 GeV, a well-known value from other quark model analysis [32,40,68]. We will leave the quark masses and smearing parameter σ and the mixing factor c_1 as externally adjustable variables. We picked a set of values for ($m_{u(d)}, m_s, m_c, m_b, \sigma, c_1$) and proceed with the following procedure to solve for the rest of parameters.

We are left with three more parameters ($a, \beta_{q\bar{q}}^P, \beta_{q\bar{q}}^V$) for mesons of a certain quark combination ($q\bar{q}$), where $\beta_{q\bar{q}}^P$,

$\beta_{q\bar{q}}^V$ are the gaussian parameters for pseudoscalar and vector mesons, respectively. Using the masses of π and ρ as our input values for $M_{q\bar{q}}$ in Eq. (9), and the condition that our coupling constants α_s are the same for all these ground state pseudoscalar and vector mesons, we can fix the three model parameters ($a, \beta_{q\bar{q}}^P, \beta_{q\bar{q}}^V$) for $q = u$ or d from the following three equations:

$$M_\pi(\beta_{q\bar{q}}^P, a) = 0.140, \quad (\text{A2a})$$

$$M_\rho(\beta_{q\bar{q}}^V, a) = 0.780, \quad (\text{A2b})$$

$$\alpha_s(\beta_{q\bar{q}}^P, a) = \alpha_s(\beta_{q\bar{q}}^V, a). \quad (\text{A2c})$$

Solving these equations not only gives us the remaining parameters $a, \beta_{q\bar{q}}^P$ and $\beta_{q\bar{q}}^V$, but also the coupling constant α_s which we assumed to be the same for all the mesons we consider here. We can then solve for the β values of all the other mesons using the known α_s value, by equating the α_s expressions for different mesons that we got from Eq. (A1). We thus fixed all parameters for the ground state pseudoscalar and vector mesons we consider here.

We then assign a different set of values to the externally adjustable variables, i.e., ($m_{u(d)}, m_s, m_c, m_b, \sigma, c_1$), and repeat the above procedure until we find a set of values that give best fit for the meson mass spectra.

Through our trial and error type of analysis, we found $m_q = 0.205$ GeV, $m_s = 0.38$ GeV, $m_c = 1.75$ GeV, $m_b = 5.15$ GeV, $\sigma = 0.423$ GeV, $c_1 = \sqrt{0.7}$ gives best fit. We then determine the mixing angles from the mass spectra of (ω, ϕ) and (η, η') using Eqs. (10) and (11) as we have described in Sec. II. In addition, the multiplicative factor λ in front of the smearing parameter σ for the ($c\bar{c}, b\bar{c}, b\bar{b}$) systems were adjusted utilizing the hyperfine splittings of (b, c) quark sectors as we have discussed in Sec. III. The updated β values with this λ adjustment are listed in Table II.

-
- [1] E. Bagan *et al.*, *Nucl. Phys. B Proc. Supp.* **54**, 208 (1997).
 [2] W. Lucha, F. F. Schöberl, and D. Gromes, *Phys. Rep.* **200**, 127 (1991).
 [3] A. De Rújula, H. Georgi, and S. L. Glashow, *Phys. Rev. D* **12**, 147 (1975).
 [4] L. A. Kondratyuk and D. V. Tchekin, *Phys. At. Nucl.* **64**, 727 (2001).
 [5] H.-Y. Cheng, C.-Y. Cheung, and C.-W. Hwang, *Phys. Rev. D* **55**, 1559 (1997).
 [6] C.-W. Hwang, *Phys. Rev. D* **81**, 114024 (2010).
 [7] P. L. Chung, F. Coester, and W. N. Polyzou, *Phys. Lett. B* **205**, 545 (1988).
 [8] F. Cardarelli, I. L. Grach, I. M. Narodetskii, G. Salme, and S. Simula, *Phys. Lett. B* **349**, 393 (1995).
 [9] P. A. M. Dirac, *Rev. Mod. Phys.* **21**, 392 (1949).
 [10] S. J. Brodsky, H.-C. Pauli, and S. Pinsky, *Phys. Rep.* **301**, 299 (1998).
 [11] S. J. Brodsky and D. S. Hwang, *Nucl. Phys. B* **543**, 239 (1999).
 [12] J. P. B. C. de Melo, J. H. O. Sales, T. Frederico, and P. U. Sauer, *Nucl. Phys. A* **631**, 574c (1998).
 [13] H.-M. Choi and C.-R. Ji, *Phys. Rev. D* **58**, 071901(R) (1998).
 [14] H.-M. Choi and C.-R. Ji, *Phys. Rev. D* **59**, 074015 (1999); *Phys. Lett. B* **460**, 461 (1999).
 [15] H.-M. Choi and C.-R. Ji, *Phys. Rev. D* **80**, 054016 (2009).
 [16] H.-M. Choi and C.-R. Ji, *Phys. Rev. D* **75**, 034019 (2007).
 [17] W. Jaus, *Phys. Rev. D* **60**, 054026 (1999).
 [18] W. Jaus, *Phys. Rev. D* **67**, 094010 (2003).
 [19] H.-Y. Cheng, C.-K. Chua, and C.-W. Hwang, *Phys. Rev. D* **69**, 074025 (2004).
 [20] H.-M. Choi and C.-R. Ji, *Nucl. Phys. A* **856**, 95 (2011); *Phys. Lett. B* **696**, 518 (2011).
 [21] J. P. B. C. de Melo and T. Frederico, *Phys. Lett. B* **708**, 87 (2012).
 [22] W. Jaus, *Phys. Rev. D* **41**, 3394 (1990).
 [23] H.-M. Choi, *Phys. Rev. D* **75**, 073016 (2007).

- [24] S. Adler and A. Davis, *Nucl. Phys. B* **244**, 469 (1984); A. Le Yaouanc, L. Oliver, S. Ono, O. Pène, and J.-C. Raynal, *Phys. Rev. D* **31**, 137 (1985); F. J. Llanes-Estrada, S. R. Cotanch, A. P. Szczepaniak, and E. S. Swanson, *Phys. Rev. C* **70**, 035202 (2004).
- [25] C. D. Roberts and A. G. Williams, *Prog. Part. Nucl. Phys.* **33**, 477 (1994); C. J. Burden, Lu Qian, C. D. Roberts, P. C. Tandy, and M. J. Thomson, *Phys. Rev. C* **55**, 2649 (1997).
- [26] H. C. Pauli and J. Merkel, *Phys. Rev. D* **55**, 2486 (1997).
- [27] H.-M. Choi and C.-R. Ji, *Phys. Rev. D* **89**, 033011 (2014); **91**, 014018 (2015).
- [28] S. J. Brodsky and G. F. de Téra mond, *Phys. Rev. Lett.* **96**, 201601 (2006); G. F. de Téra mond and S. J. Brodsky, *ibid.* **102**, 081601 (2009); G. F. de Téra mond, H. G. Dosch, and S. J. Brodsky, *Phys. Rev. D* **87**, 075005 (2013); S. J. Brodsky, G. F. De Téra mond, A. Deur, and H. G. Dosch, *Few-Body Syst.* **56**, 621 (2015).
- [29] H.-M. Choi and C.-R. Ji, *Phys. Rev. D* **77**, 113004 (2008).
- [30] S. J. Brodsky and G. F. de Téra mond, *Phys. Rev. D* **77**, 056007 (2008).
- [31] S. Capstick and N. Isgur, *Phys. Rev. D* **34**, 2809 (1986).
- [32] S. Godfrey and N. Isgur, *Phys. Rev. D* **32**, 189 (1985).
- [33] W. Jaus, *Phys. Rev. D* **44**, 2851 (1991).
- [34] S. J. Brodsky and G. P. Lepage, SLAC-PUB-1966, Invited talk presented to the Fourth International Colloquium on Advanced Computing Methods in Theoretical Physics, Saint Maximin, France, March 21–23, 1977.
- [35] G. S. Adkins and J. Sapirstein, *Phys. Rev. A* **58**, 3552 (1998).
- [36] R. Barbieri and E. Remiddi, *Nucl. Phys. B* **141**, 413 (1978).
- [37] H. A. Bethe, *Phys. Rev.* **72**, 339 (1947).
- [38] B. D. Jones, R. J. Perry, and S. D. Głazek, *Phys. Rev. D* **55**, 6561 (1997).
- [39] H. Lamm and R. F. Lebed, *J. Phys. G* **41**, 125003 (2014).
- [40] D. Scora and N. Isgur, *Phys. Rev. D* **52**, 2783 (1995).
- [41] A. M. Badalian, B. L. G. Bakker, and I. V. Danilkin, *Phys. At. Nucl.* **74**, 631 (2011).
- [42] T. Feldmann, P. Kroll, and B. Stech, *Phys. Rev. D* **58**, 114006 (1998); *Phys. Lett. B* **449**, 339 (1999).
- [43] T. Feldmann, *Int. J. Mod. Phys. A* **15**, 159 (2000).
- [44] H. Leutwyler, *Nucl. Phys. B (Proc. Suppl.)* **64**, 223 (1998).
- [45] Particle Data Group, K. A. Olive *et al.*, *Chin. Phys. C* **38**, 090001 (2014).
- [46] M. D. Scadron, *Phys. Rev. D* **29**, 2076 (1984).
- [47] R. J. Dowdall, C. T. H. Davies, T. C. Hammant, and R. R. Horgan (HPQCD Collaboration), *Phys. Rev. D* **86**, 094510 (2012).
- [48] T. Frederico, H.-C. Pauli, and S.-G. Zhou, *Phys. Rev. D* **66**, 116011 (2002).
- [49] R. Escribano and J.-M. Frere, *J. High Energy Phys.* **06** (2005) 029.
- [50] J. Schechter, A. Subbaraman, and H. Weigel, *Phys. Rev. D* **48**, 339 (1993).
- [51] D. Becirevic, Ph. Boucaud, J. P. Leroy, V. Lubicz, G. Martinelli, F. Mescia, and F. Rapuano *et al.*, *Phys. Rev. D* **60**, 074501 (1999).
- [52] S. Aoki *et al.*, FLAG Working Group, *Eur. Phys. J. C* **74**, 2890 (2014).
- [53] D. Bečirević, G. Duplanić, B. Klajn, B. Melić, and F. Sanfilippo, *Nucl. Phys. B* **883**, 306 (2014).
- [54] D. Becirevic, V. Lubicz, F. Sanfilippo, S. Simula, and C. Tarantino, *J. High Energy Phys.* **02** (2012) 042.
- [55] P. Gelhausen, A. Khodjamirian, A. A. Pivovarov, and D. Rosenthal, *Phys. Rev. D* **88**, 014015 (2013); **89**, 099901(E) (2014); **91**, 099901(E) (2015).
- [56] G. Cvetić, C. Kim, G.-L. Wang, and W. Namgung, *Phys. Lett. B* **596**, 84 (2004).
- [57] S. Capstick and S. Godfrey, *Phys. Rev. D* **41**, 2856 (1990).
- [58] D. Ebert, R. Faustov, and V. Galkin, *Phys. Lett. B* **635**, 93 (2006).
- [59] K. W. Edwards *et al.* (CLEO Collaboration), *Phys. Rev. Lett.* **86**, 30 (2001).
- [60] B. Colquhoun, R. Dowdall, C. Davies, K. Hornbostel, and G. Lepage, *Phys. Rev. D* **91**, 074514 (2015).
- [61] Belle Collaboration, K. Ikado *et al.*, *Phys. Rev. Lett.* **97**, 251802 (2006).
- [62] J. P. Lansberg and T. N. Pham, *Phys. Rev. D* **75**, 017501 (2007).
- [63] M. A. Ivanov, J. G. Korner, and P. Santorelli, *Phys. Rev. D* **63**, 074010 (2001).
- [64] D. Ebert, R. N. Faustov, and V. O. Galkin, *Phys. Rev. D* **67**, 014027 (2003).
- [65] E. J. Eichten and C. Quigg, *Phys. Rev. D* **49**, 5845 (1994).
- [66] S. S. Gershtein, V. V. Kiselev, A. K. Likhoded, and A. V. Tkabladze, *Phys. Rev. D* **51**, 3613 (1995).
- [67] L. P. Fulcher, *Phys. Rev. D* **60**, 074006 (1999).
- [68] N. Isgur, D. Scora, B. Grinstein, and M. B. Wise, *Phys. Rev. D* **39**, 799 (1989).